International Specialty Conference on Cold-Formed Steel Structures

Wei-Wen Yu International Specialty Conference on Cold-Formed Steel Structures 2018

Nov 7th, 12:00 AM - Nov 8th, 12:00 AM

Transverse Shear Stiffness of Bolted Cold-Formed Steel Storage Rack Upright Frames with Channel Bracing Members

Nima Talebian

Benoit P. Gilbert

Hassan Karampour

Wei-Wen Yu International Specialty Conference on Cold-Formed Steel Structures
St. Louis, Missouri, U.S.A., November 7 & 8, 2018

Transverse shear stiffness of bolted cold-formed steel storage rack upright frames with channel bracing members

Nima Talebian[1], Benoit P. Gilbert[1], and Hassan Karampour[1]

Abstract:

Accurately evaluating the transverse shear stiffness of cold-formed steel storage rack upright frames is crucial to calculate the frame elastic buckling load, perform earthquake design and serviceability checks. This is especially essential for high-bay racks, which are subjected to large second-order effects, and racks supporting the building enclosure, which are exposed to transverse wind loads. The shear behaviour of these frames is poorly understood and experimental testing is usually required to measure their stiffness. Previous studies have shown that Finite Element Analyses (FEA), solely using beam elements, fail to reproduce experimental test results and may overestimate the transverse shear stiffness by a factor up to 25. In this paper, a commercially used upright frame, with either bolted lip-to-lip or back-to-back channel section bracing members, has been modelled using shell elements. The model is verified against available experimental data and found to accurately predict the experimental shear stiffness with an average error of 7%. Based on the verified FE model, the factors contributing to the frame shear deformation are quantified. The different frame deformations imposed by the test set-ups in the European (EN15512) and Australian (AS4084) standards are both considered. The effects of the bracing lay-out, the bolt bending, local deformations of the uprights and bracing members at the connections on the performance of the upright frames are quantified and discussed.

Keywords: Steel storage racks, Cold-formed steel, Upright frames, Shear stiffness, Finite Element Analysis

Introduction

Steel storage rack systems, commonly assembled from cold-formed steel profiles, are extensively used in industry to store goods. Goods are placed on pallets which are positioned on the racks using forklift trucks. They act as freestanding structures and are designed as lightly as possible, while still capable of carrying heavy loads (Gilbert et al., 2012). Their popularity lies in their ability to increase storage capacity by both minimising the floor space and providing a number of different storage configurations (Freitas et al., 2005). The most common type of rack is referred to as “selective” storage rack and typically consists of uprights, pallet beams, bracing members and connectors, as illustrated in Fig. 1. In the down-aisle direction, the stability of unbraced racks is solely ensured by the base plate-to-floor and pallet beam-to-upright semi-rigid connections (Bajoria et al., 2010; Davies 1980; Godley and Beale, 2008; Gilbert and Rasmussen, 2011). In the cross-aisle direction, the stability is ensured by the upright frames, each consisting of two uprights connected by bracing members, as shown in Fig. 1 and Fig. 2. The bracing members are commonly cold-formed lipped channel-sections bolted to the upright flanges. Welded connections are also encountered. Other forms of cold formed profiles, such as circular hollow sections, are also used in practice.

Although, the configuration of steel storage rack structures is simple, as they are assembled from beams, uprights and bracings, their analysis and design are complicated. Due to the nature of the cold-formed steel elements, their performance is influenced, among others, by local deformations at the uprights and bracing members at the connections (Sajja et al, 2008). The base plate-to-floor and beam-to-upright semi-rigid connections also influence the structural behaviour of the system (Baldassino and Bernuzzi 2000; Prabha et al., 2010).

The transverse shear stiffness of the upright frames has a significant impact on the behaviour of the overall structure in the cross-aisle direction. As rack structures are sensitive to second order effects,

[1] School of Engineering and Built Environment, Griffith University, Gold Coast, Australia

precisely determining the shear stiffness is of a great importance for serviceability checks, and to calculate the elastic buckling loads and earthquake design forces. This is especially relevant for high-bay racks that can reach heights greater than 20 metres and racks supporting the building enclosure which are subjected to cross-aisle horizontal forces due to wind loading. The shear behaviour of the upright frames is currently poorly understood and investigations are still needed to advance the knowledge.

Currently, different approaches are adopted by the three main international storage rack design specifications AS408 (2012), EN15512 (2009) and RMI (2012) to determine the shear stiffness of cold-formed steel storage rack upright frames. Timoshenko and Gere's (1961) theory is used in the Rack Manufacturers Institute specification (RMI 2012) in which the upright frame shear deformation is assumed to purely arise from the axial deformation of the bracing members. In the European design specification (EN15512 2009), experimental testing of the frame in the longitudinal direction is proposed to determine the stiffness per unit length. The test set-up consists of an upright frame restrained from rigid body rotation and with at least two bracing panels. One of the uprights is pinned at one end and a longitudinal force F is applied at the opposite end of the other upright through its centroidal axis, as depicted in Fig. 3. The longitudinal displacement of the upright, on which the force is applied, is recorded and the slope k_{ti} of the linear part of the experimental load-displacement curve is calculated. The stiffness k_{ti} is then used in conjunction with Timoshenko and Gere's (1961) theory to estimate the upright frame transverse shear stiffness S_{ti} as,

$$S_{ti} = \frac{k_{ti} d^2}{h} \tag{1}$$

where d is the distance between the centroidal axes of the two uprights and h is the height of the frame.
The Australian Standard AS4084 (2012) proposes the use of the testing method suggested by the European design specification EN15512 (2009) and an alternative approach in which the frame is loaded in the transverse direction to evaluate the combined shear and bending stiffness, as shown in Fig. 4. In the alternative approach, the frame is composed of a minimum number of two bracing panels. The bottom ends of the uprights are pinned to a rigid frame and the top ends of the uprights are prevented from out-of-plane displacements. A load F is applied to the frame at the elevation of the top horizontal bracing member. Two displacement transducers are positioned at the elevations of the top (i.e. where the load F is applied) and bottom horizontal bracing members. The combined bending and shear transverse stiffness S_{cti} is then calculated as,

$$S_{cti} = k_{cti} h \tag{2}$$

where k_{cti} is the slope of the experimental load-displacement curve, with the displacement being calculated as the difference between the two transducers, and h is height of the frame.

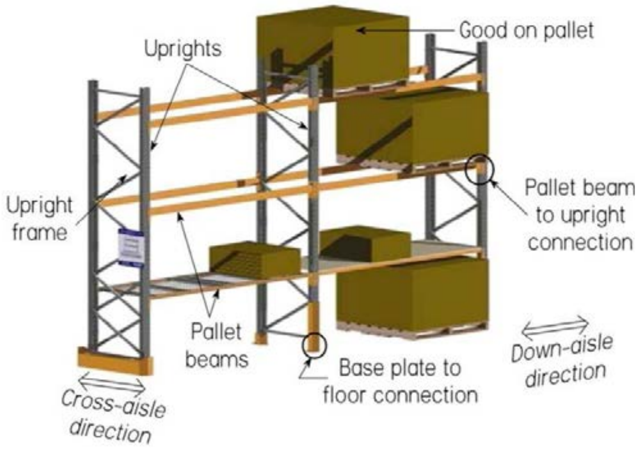

Fig. 1. Elements of a typical rack structure (Gilbert et al., 2012)

Very limited studies have investigated the transverse shear stiffness of cold-formed steel storage rack bolted upright frames. Rao et al. (2004), Sajja et al. (2008) and Sajja (2010) experimentally and numerically investigated the shear stiffness of various upright frames. Developed models with beam elements which included upright bending stiffness, the eccentricity of bracing members and the bending of the bolt connecting the bracings to the upright, were not able to successfully reproduce the experimental test results. The models overestimated the shear stiffness by a factor of 2 to 5. The discrepancy was attributed to the “torsional distortion” of the uprights, not being considered in the model. It was recommended that it is essential to consider the contact behaviour between various elements at the connections to accurately determine the shear stiffness.

Gilbert et al. (2012) performed 36 tests of bolted upright frames following both the EN15512 (2009) and alternative AS4084 (2012) test set-ups. The two methods were compared and the practical use of the alternative method proposed by the AS4084 was demonstrated. The conclusions were based on three upright section types and two different bracing cross-sections (CHS and channels), totalling six different upright frame types. Finite Element models were also developed in Gilbert et al. (2012) using beam elements. The analyses overestimated the upright frame shear stiffness by a factor of 9 to 25 for the test set-up in the EN15512 (2009) and 3 to 16 for the alternative test set-up in the AS4084 (2012). This difference was mainly attributed to the local deformation of the connections between bracing members and uprights, not being considered in the model.

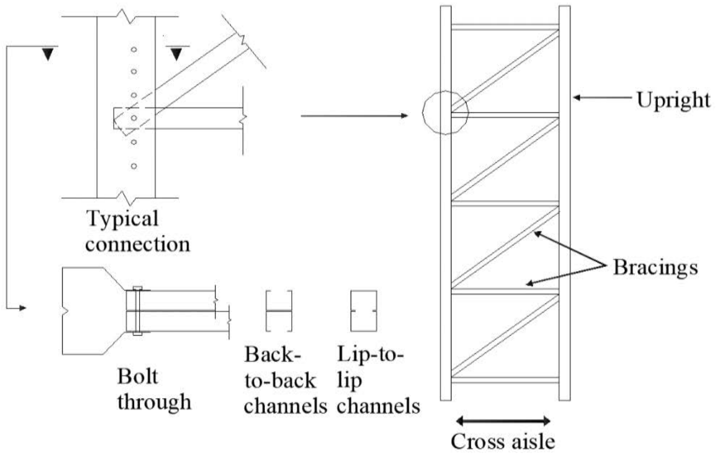

Fig. 2.Typical upright frame

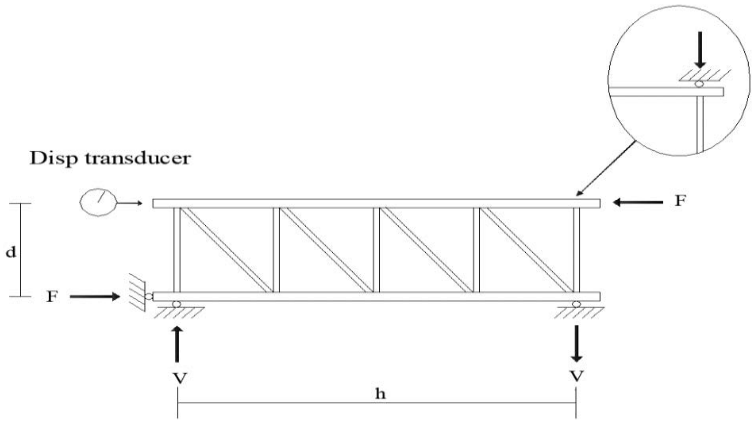

Fig. 3. Upright frame shear stiffness test set-up EN15512 (2009)

Far et al. (2017) numerically and experimentally investigated the shear behaviour of the upright frames. Developed FE models of the upright frames using solid elements overestimated the shear stiffness by 30%. A simplified modelling approach was also proposed to account for the flexibility in bolted connections. Roure et al. (2016) experimentally and analytically studied the behaviour of upright frames. Tests were performed on the joints between uprights and braces as well as on the upright frames. A simple practical design approach was proposed based on an adjusted cross-sectional area at both ends of the bracing members to consider that the axial stiffness of the bracing members is affected by the local distortions at the joints.

To understand all factors affecting the transverse shear behaviour of bolted cold-formed steel storage rack upright frames, numerical models that are able to capture the deformations at the bolted connections are required (Gilbert et al., 2012; Sajja et al., 2008; Sajja (2010). This paper develops and details an advanced Finite Element (FE) model of a commercially used upright frame, with either bolted lip-to-lip or back-to-back channel section bracing members to accurately predict the transverse shear stiffness of storage rack upright frames. The accuracy of the model is verified against experimental tests performed on upright frames in Gilbert et al. (2012) and tested following the two different set-ups. The various factors influencing the shear stiffness of the rack upright frames with lip-to-lip and back-to-back channel bracing members are then numerically identified, quantified and discussed. These results would provide rack manufacturers the possibility to improve their design by targeting the factors influencing the most the shear stiffness of the frames.

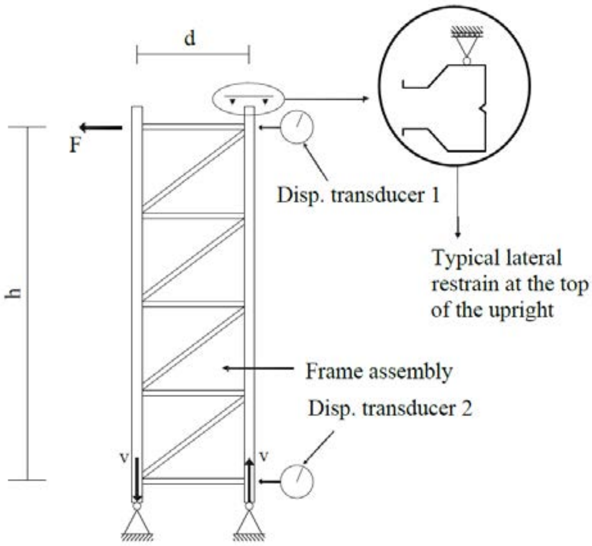

Fig. 4. Alternative test set up AS4084 (2012)

Experimental tests used to verify FE models

As mentioned in the Introduction, Gilbert et al. (2012) tested upright frames assembled from three upright types (A, B and C) and with two bracing configurations: circular hollow sections in a X-pattern and lip-to-lip Cannel sections in a Z-pattern to determine both the shear stiffness S_{ti} (Eq (1)) and the combined transverse bending and shear stiffness, S_{cti} (Eq (2)). In total 17 tests were performed with channel bracing members. The upright frames were tested following both the EN15512 (2009) and the alternative AS4084 (2012) test set-up procedures. Three repeat tests have been performed per upright frame configuration. When Type A upright frame following the EN15512 (2009), only two tests were performed. In this paper, only the configuration with the smallest upright type (Type A) with lip-to-lip channel-sections bracing members in a Z-pattern as shown in Fig. 5, is used to validate the FE model. These upright frames were tested with bracing type C35x20x1.2. The main dimensions of the Type A upright is shown in Fig. 6 and the cross-sectional properties of the upright and bracing member are presented in Table 1. End plates were welded to the ends of the uprights to ensure easy connection and restrain warping. For the frames tested following AS4084 (2012) displacements were recorded at each bracing elevation, from LVDT 4 at the bottom bracing elevation to LVDT 1 at the top bracing elevation.

The test set-ups for the upright frame tested following the alternative method in the AS4084 (2012) is shown in Fig. 7 (a). The frames were restrained from lateral out-of-plane displacements at six locations along the height of the frame, as depicted in Fig. 7 (a). Fig. 7 (b) and (c) shows the vertical restraint and their schematic view, respectively. Bottom Nylon pads sprayed with silicone were placed underneath the uprights so as to allow the horizontal displacement of the frame. The top Nylon pads were pinned above the centroid axis of the uprights. Specifically, the latter pads were loosely connected to steel square hollow sections (SHS) using steel balls to both avoid out-of-plane movement and allow the uprights to rotate. The supported steel SHS in Fig. 7 were bolted to the strong floor through threaded bars.

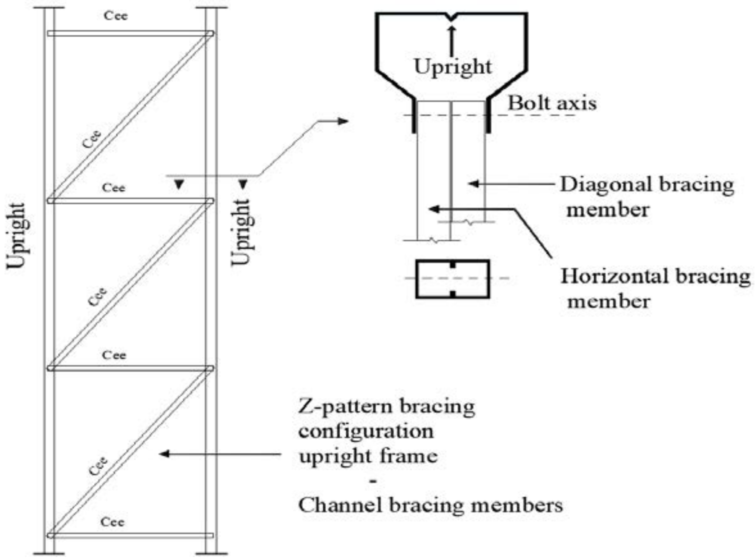

Fig. 5. Z-pattern bracing configuration with channel bracing members

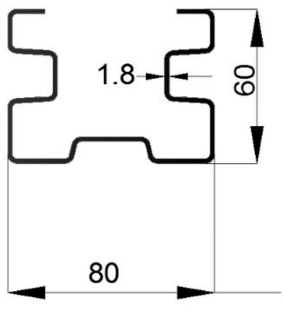

Fig. 6. Main dimensions of the upright in mm

Table 1 : Cross-sectional properties of the upright and bracing member

Member	Gross area (mm^2)	$I_{major\ axis}$ (mm^4)	$I_{minor\ axis}$ (mm^4)	J (mm^4)	$I_{warping}$ (mm^6)
Upright	484.0	4.34×10^5	1.91×10^5	491.9	2.21×10^8
C35 × 20 × 1.2	100.0	1.83×10^4	4.60×10^3	47.5	1.79×10^6

Finite element modelling

A FE model built using the Finite Element software ABAQUS (2015) is detailed hereafter to capture both the global and local deformations of the upright frame.

Due to the loose connection between the top Nylon pads and the uprights (Fig. 7), the influence of the top pads on FE response can be physically ignored for the upright frames tested following the alternative method in the AS4084 (2012) and the method in the EN15512 (2009). Only bottom Nylon pads were consequently modelled in the FEA simulations and fixed to the ground. The interaction between the uprights and bottom pads was modelled using a frictionless surface-to-surface contact. During tests, upright frames rotate and displace towards the bottom Nylon pads and remain in contact with them. Therefore, only modelling the bottom pads is enough to prevent out-of-plane displacements and this was found to accurately represent the effect of vertical restraint on the frame response, as detailed in previous section. Fig. 8 shows the details of the vertical restraints used in the FE models.

Reduced integration four node shell elements, S4R, were used to model the uprights, upright end plates and bracing members at their wall center-line. Only largest perforations of the uprights were considered in the FE model. Bolts and pinned supports were modelled using C3D10 solid elements. Based on convergence studies performed on a single upright and bracing member, the size of the S4R elements was found to be about 10 mm × 15 mm for the uprights and 10 mm × 10 mm for the bracing members to well capture the frame deformation. In the vicinity of the bolted connections, 3 mm × 3 mm mesh size was found to be fine enough to accurately capture the local deformations of the connections. The mesh size was further refined locally around the bolt holes to account for the presence of stress concentrations (Kim and Kuwamura, 2007). Five integration points through the thickness of the shell elements were considered.

To replicate the actual behaviour at the bolted connections, the interaction between elements was modelled using contacts elements. Especially, the contacts between (i) the bolts and the bolt holes, and (ii) upright flange edges and bracing webs were modelled using the node-to-surface discretization method, with small sliding and zero initial clearance. Consequently, the looseness in the connections was ignored. The contacts between (i) the bracing members and upright flanges, and (ii) the bolt head/nut and uprights were simulated using the surface-to-surface discretization method with finite sliding. Hard contact with friction coefficient equal to 0.3 was considered as interaction behaviour for all contacts. The bracing members were assumed to fit perfectly between the upright flanges, i.e. no gap was considered between these elements.

The material non-linearity was modelled using the von Mises yield criteria and isotropic hardening. The stress-strain curves were inputted into ABAQUS (2015) as multi-linear curves and derived from tensile coupons cut from the uprights and bracing members. To account for the change of cross-sectional dimensions of the coupons during testing, true engineering stress and strain were employed in the numerical model.

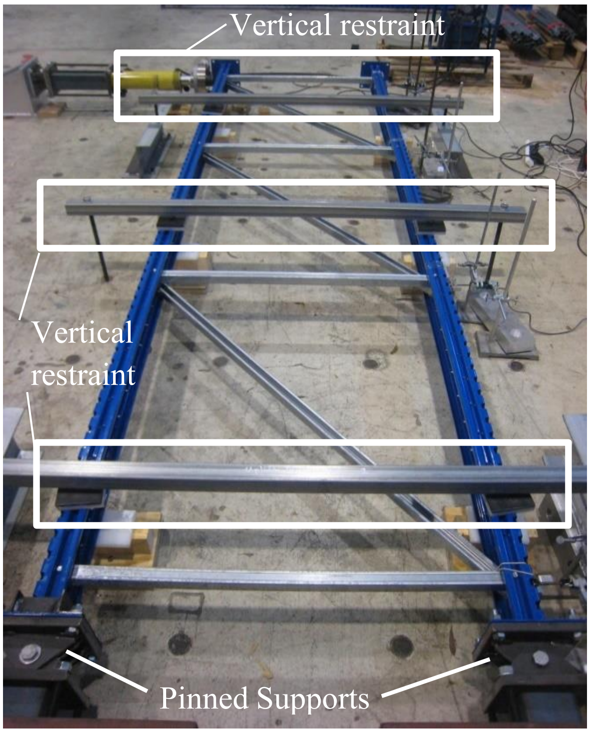

(a)

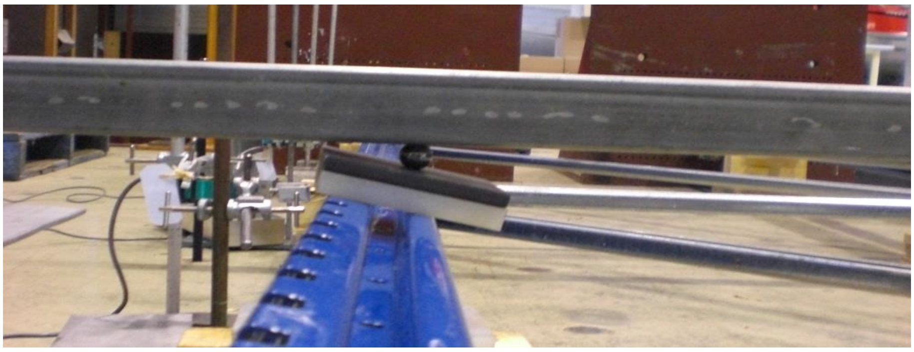

(b)

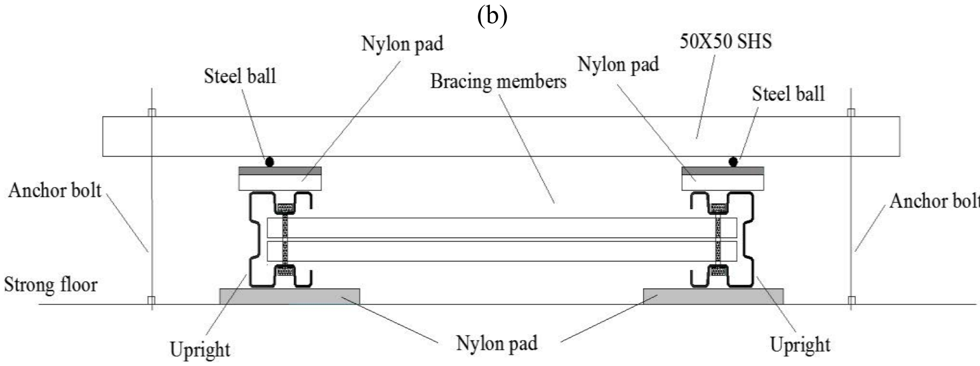

(c)

Fig. 7. Test set-up performed for the upright frame following the alternative method in AS4084 (2012) (a) overall view of the upright frame (b) vertical restraint during test (c) schematic view of the vertical restraints

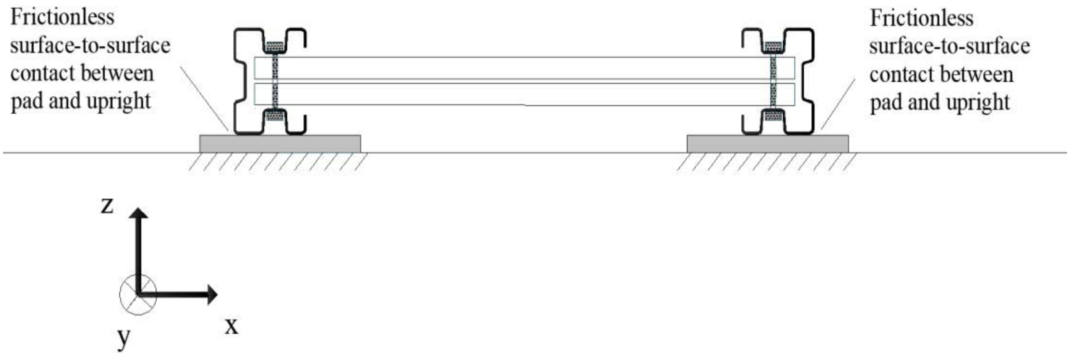

Fig. 8. Vertical restraint used in FE model for the upright frames

Validation of the FE model and comparison with experimental results

To consider all deformations occurring in the frames, nonlinear geometry and material analyses were ran. Yielding at the bolt holes were found to occur at an early stage of loading (particularly for the frames tested following the alternative AS4084 test set-up) and this is captured by the FEA. As the paper focuses on the initial shear stiffness of the frames, analyses were stopped when the applied load reached about 67% (AS4084 test set-up) and 60% (EN15512 test set-up) of the experimental failure load.

Tests following the AS4084 test set-up

Fig. 9 compares the load-deflection curves (deformation taken as the difference between the displacements at the top and bottom bracing elevations - Fig. 4) between FEA and experimental test results for the upright frame. Table 2 gives the stiffness k_{cti} (Eq. (2)) calculated from both the FEA and experimental results. The stiffness are calculated by performing a linear regression on the load-deflection curves, i.e. between 1 kN and 3 kN. Fig. 9 and Table 2 show a reasonable agreement between the FEA and experimental tests. The difference in stiffness is 6%. Fig. 10 compares the displacements recorded by all LVDTs (i.e. at all bracing elevations) with FEA results for the 1st test performed on the upright frame. The FEA is able to well predict the overall frame displacement.

Fig. 11 compares the FE deformation of the frame to available experimental photos of the tested upright frame. The developed FE model predicts well the overall deformed shape. Note, to magnify the deformation of the frame, Fig. 11 is shown at a FE displacement greater than the one shown in Fig. 9.

Tests following the EN15512 test set-up

Fig. 12 compares the load-deflection curves, at the load application point of the EN15512 test set-up, between the FEA and experimental test results for the upright frame. Table 2 gives the stiffness k_{ti} (Eq. (1)) calculated for both the FEA and experimental results. In Table 2, the stiffness were determined by performing a linear regression on the load-deflection curves between 5 kN and 12 kN for the upright frame. Fig. 12 and Table 2 show a good agreement between the FEA and experimental tests. The predicted to experiment ratio is 1.07.

Fig. 13 presents the deformed shape of the FEA and experimentally tested upright frame and shows that the developed FE model predicts well the overall deformed shape. Note, to magnify the deformation of the frame, Fig. 13 was shown at a FE displacement greater than the one shown in Fig. 12.

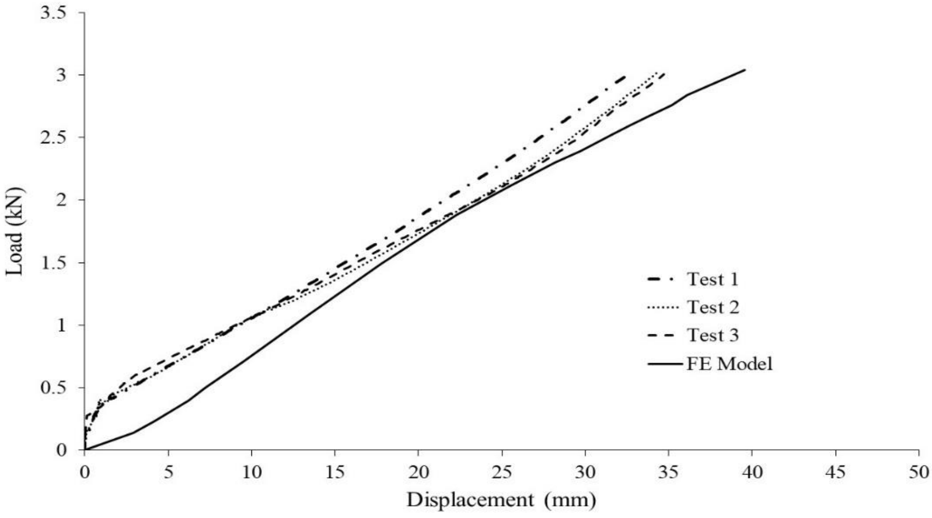

Fig. 9. FEA and experimental load-deflection curves for AS4084 (2012) test set-up

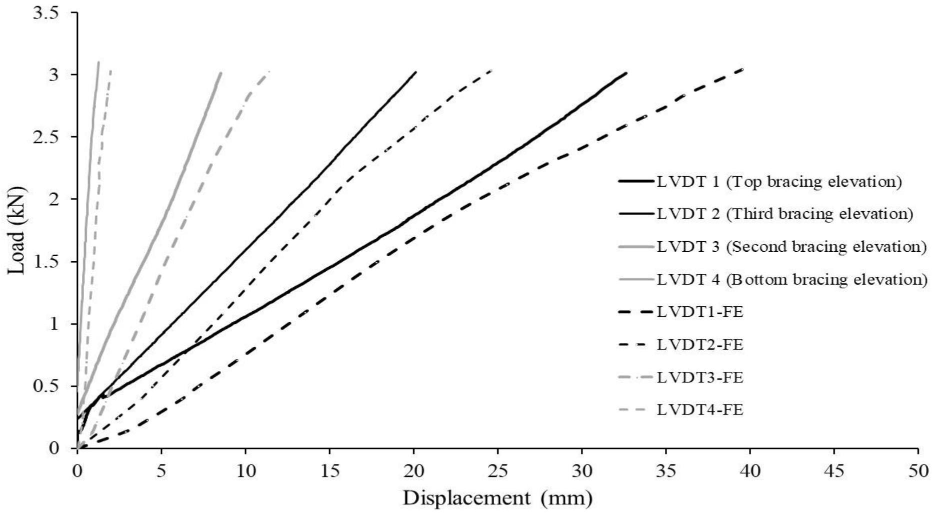

Fig. 10. FEA and experimental load-deflection curves for all LVDTs and AS4084 (2012) test set up

Contribution of factors affecting the transverse shear stiffness

The verified FE model is used herein to determine the contribution of factors affecting the shear stiffness of the Type A upright frames. The following factors are investigated (a) bolt bending deformation, (b) local deformation at the bracing member bolt holes, (c) local deformation at the upright bolt holes (d) cross-sectional deformation of the end of the bracing members, (e) cross-sectional deformation of the uprights in the vicinity of the bolted connection, (f) axial elongation of bracing members and (g) upright overall bending and shear deformation.

Table 2: Transverse shear stiffness for FEA and experimental tests

	AS4084 (2012) k_{Cti}	EN215512 (2009) k_{ti}
FEA (kN/mm)	0.084	1.22
Experiment (kN/mm)	0.089	1.14
FEA/Exp	0.94	1.07
Difference (%)	6	7

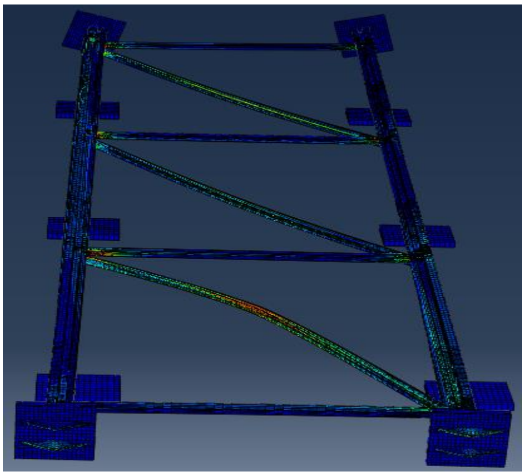

(a) (b)

Fig. 11. Deformed shapes following the AS4084 (2012) test set-up (a) FEA (with deformed scale factor of 1.0 and at a displacement of 70 mm) and (b) experimental observations

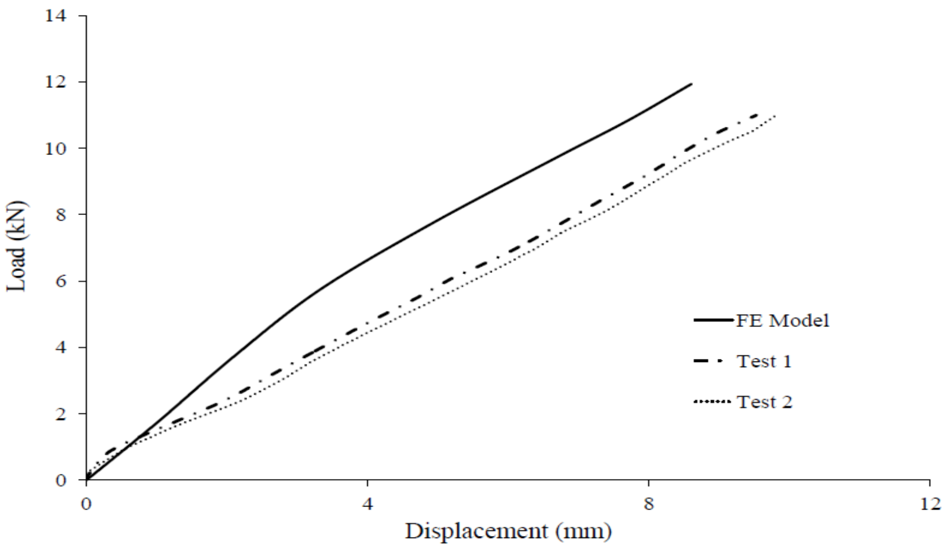

Fig. 12. FEA and experimental load-deflection curves for EN15512 (2009) test set-up

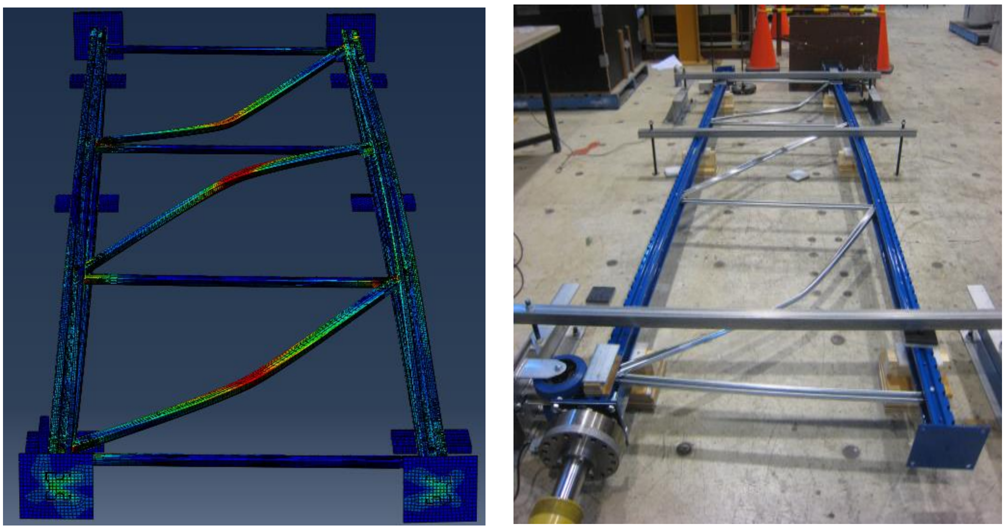

(a) (b)

Fig. 13. Deformed shapes following the EN15512 (2009) test set-up (a) FEA (with deformed scale factor of 1.0 and at a displacement of 14 mm) and (b) experimental observation

Specifically, the contribution of the previous factors were determined by performing the following changes to the FE model:

(a) *Bolt bending deformation*: the bending stiffness of the bolts was increased by multiplying their Young's modulus E by 100 (Yu and Schafer, 2007), effectively creating rigid bodies.

(b) *Local deformation at bolt hole of bracing members*: a 2 mm wide circular strip around the upright holes was modelled with a high Young's modulus (multiplied by 100). This strip width was found to be efficient in preventing ovalization of the holes.

(c) *Local deformation at bolt hole of uprights*: Similar to (b), a 2 mm wide circular strip around the holes was modelled with a high Young's modulus (multiplied by 100).

(d) *Cross-sectional deformation of bracing members*: to prevent the cross-sectional deformation of the bracing members at the bolted connections (as in Figs 19 (d) and 24 (b)), the ends of the bracing members were made rigid, by increasing their Young's modulus by a factor of 100, on a length of 70 mm.

(e) *Bracing axial deformation*: the Young's modulus of the entire bracing members was increased by 100 to prevent their axial shortening and elongation.

(f) *Cross-sectional deformation of uprights*: to prevent the cross-sectional deformation of the uprights at the connections, the Young's modulus of the uprights on a length of +/- 75 mm about the bolted connection, was multiplied by 100.

(g) *Upright shear and bending deformation*: similar to (e) the Young's modulus of the entire upright was multiplied by 100, so the uprights act as rigid bodies.

The contribution of the deformations of bracing members and uprights to the overall shear stiffness of the upright frames is treated separately in this paper. The combinations of factors analysed are presented in Table 3. Note that while the influence of the upright and bracing member deformations are treated separately, preventing the bracing members to deform would have an influence on the local deformation of the uprights. The same applies to the local behaviour of the bracing members when preventing the uprights to deform.

Similarly to the model presented earlier, nonlinear geometry and material analyses are performed with the same material properties. The influence of each analysed factor on the overall shear stiffness is quantified as:

$$\Omega = \frac{S_{modified}}{S_{initial}} \tag{3}$$

where $S_{initial}$ and $S_{modified}$ are the initial numerical (reported in Table 2) and modified (i.e. with increased E for selected parts of the frame) shear stiffness of the upright frames, respectively, calculated from Eqs (1) and (2) for the EN15512 and AS4084 test set-ups, respectively.

The modelled upright frame tested in Gilbert et al. (2012) with lip-to-lip channel bracing members is used as a case study in the paper. In addition, to further analyse the behaviour of the frames, the previous analyses were re-run with back-to-back channel bracing members. The contribution of the aforementioned factors is analysed for these frames for both the AS4084 and EN15512 test set-ups.

Contribution of factors affecting the transverse shear stiffness of lip-to-lip upright frames

Contribution of factors according to AS4084 test set-up

Table 3 shows the contribution of the analysed factors on the shear stiffness of Type A upright frame following the AS4084 test set-up and lip-to-lip bracing configuration. The effect of the bolt bending on the frame shear stiffness is about 2%. This results from the load mainly being transferred in shear in the bolt from the web of the bracing members to the uprights (Sajja et al., 2008; Far et al., 2017).

From Table 3, the effect of the local deformation at the bracing holes contributes about 14% to the shear stiffness. This is observed in the FEA by plastification occurring at the bracing holes earlier for the upright frame. The cross-sectional deformation at the ends of the bracing members is found to significantly contribute to the shear stiffness of the frame, with the stiffness being increased by more than 50%. This is attributed to the upright type being a compact cross-section, therefore not prone to cross-sectional deformation. The axial stiffness of the bracing members was found to contribute more to the overall stiffness of the upright frame (about 12%).

Regarding the deformation of the uprights, the local deformation at the holes and the cross-sectional deformation at the connections contribute to the shear stiffness of the frame about 1% and 6% respectively. Having rigid uprights increases the shear stiffness by 57% for the upright frame.

Table 3: Contribution of factors on shear stiffness for each structural component- lip-to-lip upright frame

Structural component	Factors	Contribution (Ω) AS4084 test set-up	Contribution (Ω) EN15512 test set-up
Bolts	(a) Bolt bending	1.02	1.02
Bracing members	(b) Local deformation at the bolt holes	1.14	1.23
	(b) + (d) Local deformation at the end of braces	1.64 (+ 0.50)	1.75 (+ 0.52)
	(b) + (d) + (e) Axial deformation of braces	1.76 (+ 0.12)	1.91 (+ 0.16)
Uprights	(c) Local deformation at the bolt holes	1.01	1.02
	(c) + (f) Local deformation at the connections	1.07 (+ 0.06)	1.31 (+ 0.29)
	(c) + (f) + (g) Upright bending stiffness	1.64 (+ 0.57)	1.85 (+ 0.54)

Contribution of factors according to EN15512 test set-up

In general, when tested using the EN15512 test set-up, the analysed factors contribute to the overall shear stiffness of the frames following a similar trend than when tested following the AS4084 test set-up. For the upright frame, the local deformation of the upright affects more the overall shear stiffness when tested following the EN15512 test set-up (about 29%) than when tested following the AS4084 test set-ups (about 6%). The differences are attributed to the different loading directions between the two test set-ups, resulting in different deformations of the frames.

Contribution of factors affecting the transverse shear stiffness of back-to-back upright frames

Contribution of factors according to AS4084 test set-up

Back-to-back bracing configurations typically show higher shear stiffness than lip-to-lip bracing configurations (Sajja et al., 2008; Rao et al., 2004; Far et al., 2017). Table 4 shows the contribution of the analysed factors on the shear stiffness of the back-to-back upright frames following the AS4084 test set-up. The effect of bolt bending on the shear stiffness is significant, about 14%, due to the back-to-back bracing pattern, now, resulting in high bending moments in the bolts.

Similar to the lip-to-lip configurations, the effect of the local deformation at the bracing holes and cross-sectional deformation at the ends of the bracing members contribute to the frame shear stiffness about 12% and 30% respectively. Unlike the lip-to-lip upright frames, the axial stiffness of the bracing members is found to significantly contribute to the overall stiffness of the frame (141%), for the upright frame.

Regarding the deformation of the uprights and similar to lip-to-lip upright frames, effect of the local deformation at the holes and cross-sectional deformation at the connections contribute to the shear stiffness, about 1% and 14% respectively. Upright bending stiffness contributes the most to the shear stiffness about 55%. Compared to lip-to-lip upright frame, back-to-back frame show less local deformations of the uprights at the bolted connections.

Contribution of factors according to EN15512 test set-up

Similar to lip-to-lip upright frame, when tested using the EN15512 test set-up, the contribution of the analysed factors to the overall shear stiffness of the frames presents a similar trend as when tested following the AS4084 test set-up. When compared to the AS4084 test set-up, the local deformation at the bolt holes of the bracing members is insignificant and about 3%. The axial deformation of bracing members contributes more to the shear stiffness, about 227%, when tested following EN15512 set-up. The differences above are attributed to different deformations of the frames due to different loading directions between the two test set-ups.

Future work

The proposed FE model will be further verified against the remaining types of upright frames investigated in Gilbert et al. (2012). The models will then be used to quantify the contribution of all factors influencing the transverse shear stiffness of all tested cold-formed steel storage rack upright frames with bolted connections. The FEA will be further used to quantify the factors affecting shear stiffness of bolted upright frames with circular hollow section (CHS) bracing members.

Table 4: Contribution of factors on shear stiffness for each structural component – back-to-back upright frames

Structural component	Factors	Contribution (Ω) AS4084 test set-up	Contribution (Ω) EN15512 test set-up
Bolts	(a) Bolt bending	1.14	1.19
Bracing members	(b) Local deformation at the bolt holes	1.12	1.03
	(b) + (d) Local deformation at the end of braces	1.42 (+0.30)	1.53 (+0.50)
	(b) + (d) + (e) Axial deformation of braces	2.81 (+1.41)	3.80 (+2.27)
Uprights	(c) Local deformation at the bolt holes	1.01	1.02
	(c) + (f) Local deformation at the connections	1.15 (+0.14)	1.20 (+0.18)
	(c) + (f) + (g) Upright bending stiffness	1.70 (+0.55)	1.64 (+0.44)

Conclusion

In this paper, an advanced shell Finite Element model of bolted cold-formed steel storage rack upright frames, with channel-bracing members, was developed for both lip-to-lip and back-to-back bracing configurations. The nonlinear interaction (contact) behaviour between components at the bolted connections was modelled to capture the local deformation at these locations. Results show that the FE model is able to accurately capture the shear stiffness of the frames when compared to published experimental tests, with an average 7% difference. The model was then used to quantify the contribution of factors influencing the transverse shear stiffness of two configurations of upright frames, including the deformation of the bolts, bracing members and uprights. Analyses were ran by deforming the frame following the testing methods in the AS4084 and EN15512 specifications. Results showed that plastification at the bolt holes starts at an early stage of loading and particularly for the frames tested following the alternative AS4084 test set-up. For lip-to-lip upright frames, (i) effect of bolt bending on the shear stiffness is insignificant and is less than 2%, (ii) effect of the local deformation at the end of the bracing members is significant, about 51% on average for both the AS4084 and EN15512 test set-ups, and (iii) the upright bending stiffness contributes the most to the overall shear stiffness of the frames, about 56% on average for both the AS4084 and EN15512 test set-ups. For back-to-back upright frames, (i) bolt bending significantly influences the shear stiffness, 17% on average for the two test set-ups, (ii) unlike the lip-to-lip frames, axial deformation of bracings significantly influence the frame shear stiffness, about 184% on average for both the AS4084 and EN15512 test set-ups, and (iii) effect of upright bending stiffness on shear stiffness is significant, about 50% on average for both the AS4084 and EN15512 test set-ups.

References

Abaqus. "Abaqus ver. 6.14, user manual." Providence, U.S.A.: ABAQUS, Inc; 2015.
AS4084. "Steel storage racking." Sydney, Australia: Standards Australia; 2012.

Bajoria, K. M., Sangle, K. K., and Talicotti, R. S. "Modal analysis of cold-formed pallet rack structures with semi-rigid connections." *Journal of Constructional Steel Research*, 2010; 66(3): 428-441.

Davies, M. J. "Stability of unbraced pallet racks." 5th International Speciality Conference on Cold-Formed Steel Structures, St. Louis, Missouri, U.S.A.; 1980. p. 409–28.

EN 15512. Steel static storage systems – adjustable pallet racking systems – principles for structural design. Brussels, Belgium: European Committee for Standardization (CEN); 2009.

Far, H., Saleh A., Firouzianhaji A. "A simplified method to determine shear stiffness of thin walled cold formed steel storage rack frames. " *Journal of Constructional Steel Research*, 2017; 138: 799-805.

Freitas, A. M. S., Freitas, M. S. d. R., and Souza, F. T. d. "Analysis of steel storage rack columns." *Journal of Constructional Steel Research*, 2005; 61(8): 1135-1146.

Gilbert, B. P., Rasmussen, K. J. "Determination of the base plate stiffness and strength of steel storage racks." *Journal of Constructional Steel Research*, 2011; 67(6), 1031-1041.

Gilbert, B. P., Rasmussen, K. J., Baldassino, N., Cudini, T., and Rovere, L. "Determining the transverse shear stiffness of steel storage rack upright frames." *Journal of Constructional Steel Research*, 2012; 78, 107-116.

Godley, M., and Beale, R. "Investigation of the effects of looseness of bracing components in the cross-aisle direction on the ultimate load-carrying capacity of pallet rack frames." *Thin-Walled Structures*, 2008; 46(7): 848-854.

Kim, T. S., and Kuwamura, H. "Finite element modeling of bolted connections in thin-walled stainless steel plates under static shear." *Thin-Walled Structures*, 2007; 45(4): 407-421.

Rao SS, Beale RG, Godley MHR. Shear stiffness of pallet rack upright frames. 7th International Speciality Conference on Cold-Formed Steel Structures, Orlando, Florida, U.S.A.; 2004. p. 295–311.

RMI. Specification for the design, testing and utilization of industrial steel storage racks. Charlotte, U.S.A.: Rack Manufacturers Institute; 2012.

Roure, F., Peköz, T., Somalo, M. R., Bonada, J., Pastor, M. M., and Casafont, M.. "Design of industrial cold-formed steel rack upright frames for loads in cross-aisle direction." International Speciality Conference on Cold-Formed Steel Structures, Batimore, Maryand, U.S.A.; 2016. p. 493–507.

Sajja, S. "Cross-aisle shear stiffness of pallet rack upright frames." PhD thesis, Oxford Brooks Univesity; 2010.

Sajja, S., Beale, R., and Godley, M. "Shear stiffness of pallet rack upright frames." *Journal of Constructional Steel Research*, 2008; 64(7): 867-874.

Timoshenko SP, Gere JM. Theory of elastic stability. 2nd edition. New York, U.S.A.: McGraw-Hill Book Company, Inc; 1961.

Yu, C., and Schafer, B. W. "Simulation of cold-formed steel beams in local and distortional buckling with applications to the direct strength method." *Journal of Constructional Steel Research*, 2007; 63(5): 581-590.